High-Volumetric Performance Aligned Nano-Porous Microwave Exfoliated Graphite Oxide-based Electrochemical Capacitors

*Mehdi Ghaffari, Yue Zhou, Haiping Xu, Minren Lin, Tae Young Kim, Rodney S. Ruoff, and Q. M. Zhang**

With the fast growing demand for portable electronic devices, there has been a desire to design and fabricate miniaturized energy storage devices that can simultaneously deliver high energy and power. Since supercapacitors or electric double layer capacitors (EDLCs) fill a gap between conventional dielectric capacitors (high power density, low energy density) and batteries (high energy density, low power density), they have attracted much attention in recent years for a variety of energy storage applications ranging from memory back-up to consumer electronics to industrial power supplies.[1–3] They store electrical energy in a double layer interface that is usually composed of a very high surface area conductive material such as carbon materials and aqueous or organic electrolytes.[4] The high specific surface area allows the storage of large amounts of charge in the double layer for a given weight and volume of the device that results in the moderate energy and large power density of supercapacitors. Consequently, numerous studies have been focused on introducing new material systems with very high surface area, which provides an extensive interface between the electrode and electrolyte.[4–14]

Activation of carbon materials is one of the most widely used approaches for increasing the surface area of the carbon electrode materials.[6,7] Recently, the activation of microwave exfoliated graphite oxide (MEGO) with KOH was reported by Zhu et al. where a surface area of 3100 m^2 g^{-1} has been achieved and because of the nano-sized pores (bimodal distribution ≈1 nm and 4 nm), the new activated MEGO (aMEGO) material was named as the 'nano-porous MEGO'.[8] Indeed, this new material with high gravimetric surface area used as electrode for symmetric supercapacitor devices demonstrated very high gravimetric capacitances of 165 and 200 F g^{-1} using 1-butyl-3-methyl-imidazolium tetrafluoroborate (BMIM BF_4) and 1-ethyl-3-methyl-imidazolium bis (trifluoromethylsulfonyl) imide (EMIM TFSI) in acetonitrile (AN) as the electrolytes, respectively.[8] Nevertheless, the outstanding high surface area of newly developed electrode materials such as this aMEGO does not necessarily translate to high volumetric performance for a supercapacitor since their density is typically less than 0.5 g cm^{-3}. In other words, even though these high surface area materials may exhibit high gravimetric capacitance, and thus high energy or power densities per weight of the active material, their volumetric performance is less compelling. Volumetric performance that requires high density electrode materials is an important metric since technological demands require the design and fabrication of small scale energy storage devices.[9]

One method to overcome the low density of the carbon material based electrodes is to mechanically compress porous carbon powders for capacitor electrodes.[10–14] Such a mechanical densification process will inevitably produce micrometer-sized pores, for example, in packing the 'nano-porous MEGO' or aMEGO flakes that are micrometer-sized in lateral dimensions and several nanometers thick, as shown in the SEM images of **Figures 1** a and 1b. Consequently, the aMEGO electrodes fabricated using the normal mechanical packing method have a low density of 0.34 g cm^{-3}, well below the crystallographic density of graphite (2.2 g cm^{-3}), and thus exhibit only a moderate volumetric capacitance of 60 F cm^{-3}.[8]

More recently, Murali et al. reported on the use of high pressure to compress the aMEGO for achieving high volumetric capacitance and energy density since compression, as one of the easiest approaches, increases the bulk density of carbon materials (<0.5 g cm^{-3}).[10] By using 25 tons of compression force, a bulk density of 0.75 g cm^{-3} was obtained. The electrode

Prof. Q. M. Zhang
Department of Electrical Engineering
Materials Research Institute
The Pennsylvania State University
University Park, PA 16802, USA
Email: Qxz1@psu.edu

M. Ghaffari
Department of Materials Science and Engineering
Materials Research Institute
The Pennsylvania State University
University Park, PA 16802, USA

Y. Zhou
Department of Electrical Engineering
Materials Research Institute
The Pennsylvania State University
University Park, PA 16802, USA

Dr. H. Xu
School of Urban Development and Environmental Engineering
Shanghai Second Polytechnic University
Shanghai 201209, P. R. China

Dr. M. Lin
Materials Research Institute
The Pennsylvania State University
University Park, PA 16802, USA

T. Y. Kim, Prof. R. S. Ruoff
Department of Mechanical Engineering and Materials Science and Engineering Program
University of Texas at Austin
One University Station C2200, Austin, TX 78712, USA

DOI: 10.1002/adma.201301243

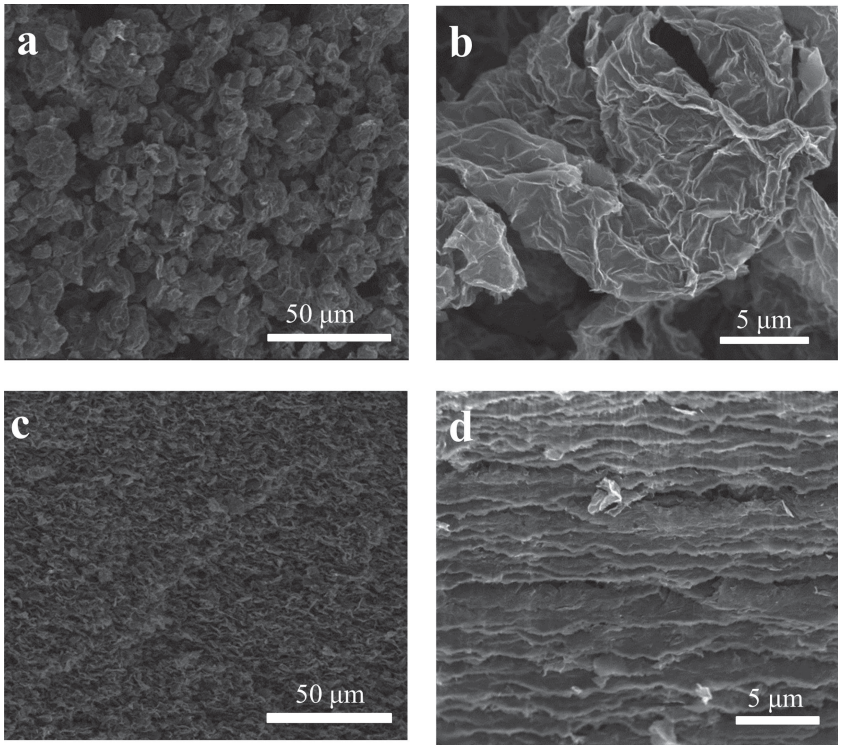

Figure 1. Low and high magnification SEM images of (a) and (b) mechanically densified aMEGO and (c) and (d) aligned aMEGO.

exhibited a high volumetric capacitance of 110 F cm^{-3} using BMIM BF_4/AN as the electrolyte at 3.5 V. Similarly, the volumetric energy density was increased from the uncompressed samples of 23 Wh l^{-1} to 48 Wh l^{-1} for the compressed samples.

In this paper, a vacuum-assisted self-assembly method was used to densify the aMEGO powder that increased the electrode density to 1.15 g cm^{-3}, significantly higher than that produced by simple compression. Very high volumetric capacitances of 158 F cm^{-3} and 177 F cm^{-3} were demonstrated for the aligned aMEGO (A-aMEGO) using BMIM BF_4/AN and EMIM TFSI/AN as the electrolytes, respectively, at 1 A g^{-1} discharge rate and 3.5 V voltage peak. A minimal reduction in the gravimetric capacitance and energy density was obtained for the A-aMEGO samples showing the enormous improvement in the volumetric values. This is attributed to the highly dense and well-ordered structure of aligned aMEGO sheets, as observed in the SEM images in Figures 1c and 1d, which provides efficient packing of the sheets while preserving the concentration and distribution of nano-sized pores, known to be responsible for charge storage.[6,11] To our knowledge, the volumetric capacitances obtained here are the highest for any activated carbon-based electrochemical capacitors reported in the literature.[3,6–8,10,12–27]

The electrochemical energy storage performance of the A-aMEGO electrodes in BMIM BF_4/AN and EMIM TFSI/AN electrolytes was evaluated using cyclic voltammetry (CV) at different scan rates and voltages. The nearly rectangular CV curves for the electrodes with BMIM BF_4/AN depicting the current and specific volumetric capacitance as a function of the applied voltage are shown in **Figure 2**. The volumetric capacitance obtained from the CV curve under 5 mV s^{-1} scan rate from 0 to 3.5 V was 155 F cm^{-3} which is much higher than other results reported to date.[8,10] This is attributed to the drastically increased density of A-aMEGO electrodes compared to similar systems. When increasing the scan rate to 20 and 100 mV s^{-1} only a slight decrease in the capacitance was observed with volumetric capacitances of 146 F cm^{-3} at 20 mV s^{-1} and 141 F cm^{-3} at 100 mV s^{-1} scan rates.

For the electrodes with EMIM TFSI/AN (Figure S1, Supporting Information) the volumetric capacitance at 5 mV s^{-1} was 175 F cm^{-3}, about three times the value reported for analogous material systems without high force mechanical compression.[8] Similar to the previous case, by increasing the scan rate to 20 and 100 mV s^{-1}, the volumetric capacitance values decreased to 163 and 157 F cm^{-3}, respectively.

To further investigate the capacitive performance of A-aMEGO electrodes, constant current galvanostatic charge/discharge cycling experiments were conducted at different discharge rates and the specific capacitance was calculated from the slope of the discharging curve after the IR voltage drop. The charge/discharge curve for the A-aMEGO electrode with BMIM BF_4/AN as electrolyte is shown in **Figure 3**a and the data obtained from the curve at 1 A g^{-1} along with the reported data for similar studies are presented in **Table 1** for comparison. The specific volumetric capacitance at 1 A g^{-1} discharge rate and a maximum voltage of 3.5 V was 158 F cm^{-3} which, consistent with the results from the CV curves, is much higher than any of the reported values (between 50 and 100 F cm^{-3}) for different types of carbon materials including activated carbon, carbon nanotubes, and even carbide-derived carbon.[3,8,10–27] Similar values were obtained for higher discharge rates of 3, 5 and 10 A g^{-1} where volumetric capacitances of 153, 149 and 147 F cm^{-3}, respectively were obtained. Similar results were collected for the electrode with EMIM TFSI/AN as shown in Figure S2 and compared in Table 1. At 1 A g^{-1} discharge rate and the same maximum voltage, the volumetric capacitance was 177 F cm^{-3}. The equivalent series resistance (ESR) values were calculated from the IR voltage drop and at 1 A g^{-1} discharge rate the ESR values were found to be 14.1 Ω and 10.8 Ω for BMIM BF_4/AN and EMIM TFSI/AN, respectively. This is consistent with the higher conductivity of EMIM TFSI compared to that of BMIM BF_4.[4]

The gravimetric electrochemical performance of electrodes, where only the mass of the active material is considered, has been widely used to compare different active material performances.[1,4–12] It is noted that in supercapacitor electrodes, besides the active materials, such as porous carbon, also the electrolyte is present. When the densities of the active materials in the electrodes do not differ noticably (the traditionally carbon based electrodes have a density of ≈0.5 g cm^{-3}), a comparison of the electrode performance in terms of per weight of pristine active material (gravimetric capacitance, energy density, and

Adv. Mater. **2013**,
DOI: 10.1002/adma.201301243

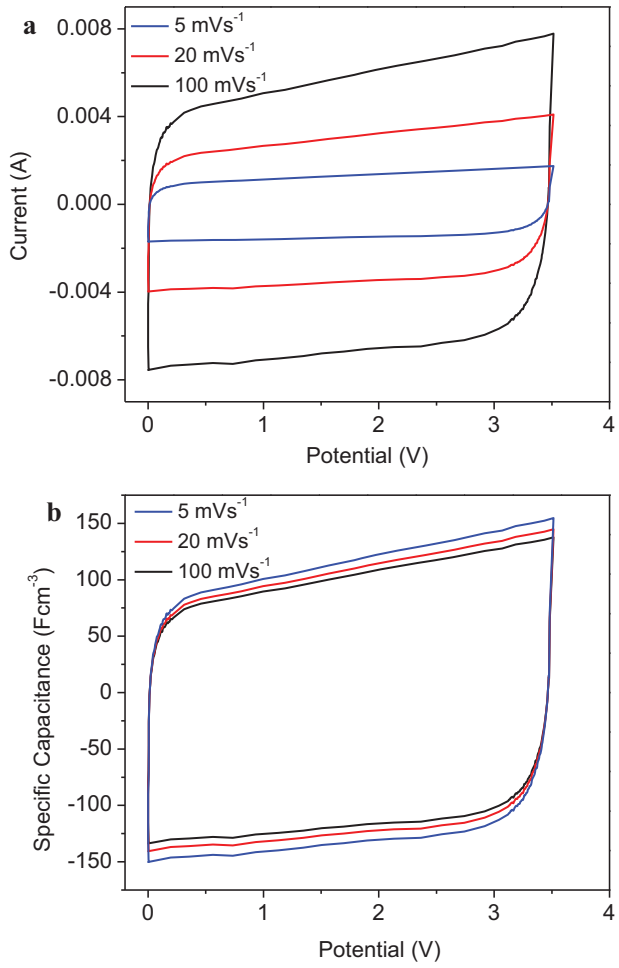

Figure 2. Cyclic voltammetry curves for A-aMEGO samples with BMIM BF_4/AN as electrolyte. (a) Current and (b) volumetric capacitance as a function of applied voltage.

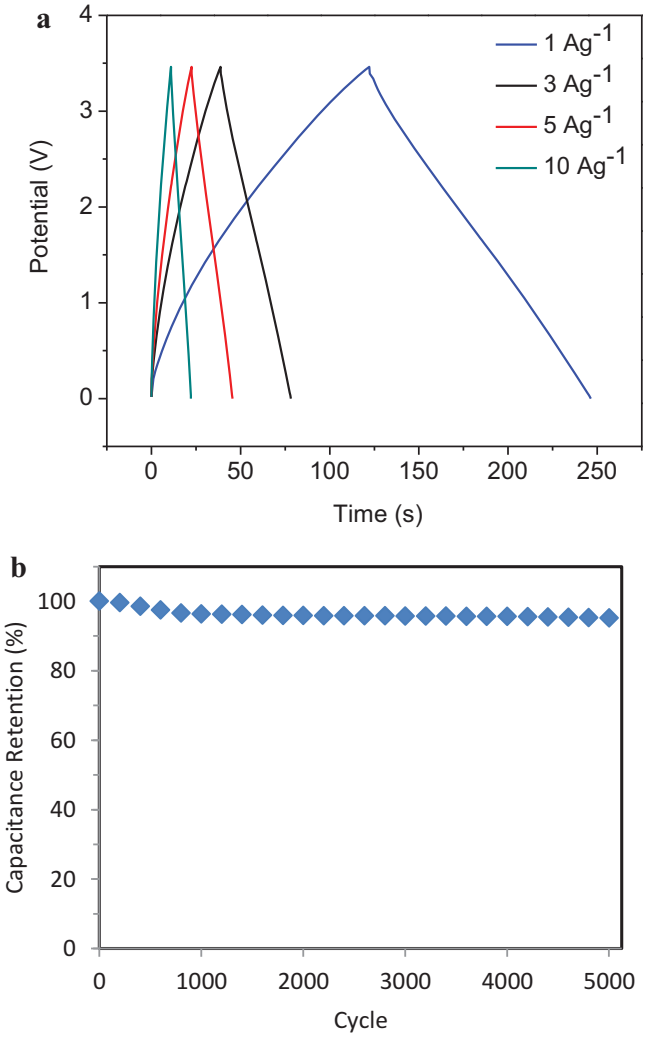

Figure 3. (a) Galvanostatic charge/discharge curve under different constant currents and a maximum voltage of 3.5 V for the A-aMEGO sample with BMIM BF_4/AN. (b) Capacitance retention test after 5000 cycles for the same sample. Retention of 94% was obtained.

power density) is meaningful.[11] Nevertheless, for electrodes with large difference of active material density, a comparison of the electrode performance based on per weight or volume of the entire electrode will provide a more realistic picture of the real device performance. For instance, regarding electrodes with an active material density of 0.34 g cm^{-3}, on the one hand, the electrode density including BMIM BF_4/AN (0.95 g cm^{-3}density) is actually 1.14 g cm^{-3}.[8] Consequently, only a small portion of the mass contributes to the energy storage. On the other hand, the density of the A-aMEGO electrode including BMIM BF_4/AN is 1.60 g cm^{-3}. Hence, a specific gravimetric capacitance of 165 F $g^{-1}$for the low density aMEGO using the active material alone, as reported earlier,[8] translates to a gravimetric capacitance of 49.2 F g^{-1} when the total electrode weight, including both the active material and electrolyte, is used. In contrast, for the A-aMEGO electrode possessing an active material density of 1.15 g cm^{-3}, a gravimetric capacitance of 154 F g^{-1} for the active material alone is equivalent to a 110.7 F g^{-1} when including the entire electrode mass. In this paper, the gravimetric values of both the active material (ACT) and the electrode (ELD) are used to distinguish between these two gravimetric values of an electrode. As shown in Table 1, there is a close correlation between the specific gravimetric performance in terms of the entire electrode weight and the specific volumetric performance. The results also indicate the importance of the volumetric performance of a supercapacitor as a more meaningful device parameter for practical applications rather than the gravimetric performance in terms of the active material only.

As shown in Table 1, the gravimetric results of ACT for A-aMEGO samples are slightly lower than the reported values for similar electrode systems with lower densities.[8] This trend indicates that the presence of the macro- sized -pores in the low density aMEGO electrodes facilitates the ion transport. Therefore, it becomes evident that the gravimetric accessible surface area per active material for a given discharge rate is higher than the high density A-aMEGO electrodes studied here. Compared to the low density aMEGO or mechanically compressed samples, the average pore size is reduced in the A-aMEGO electrodes as a result of efficient packing of graphene sheets during the self-assembly process.[8,10, 28] This efficient packing

Table 1. Comparison on gravimetric and volumetric performance of A-aMEGO samples with lower density aMEGO electrodes.

Sample	Active Material Density [g cm^{-3}]	Gravimetric Capacitance at 1 A g^{-1} (per active material weight) [F g^{-1}]	Gravimetric Capacitance at 1 A g^{-1} (per whole electrode weight) [F g^{-1}]	Volumetric Capacitance at 1 A g^{-1} (per active material weight) [F cm^{-3}]	Gravimetric Energy Density (per active material weight) [Wh kg^{-1}]	Gravimetric Energy Density (per whole electrode weight) [Wh kg^{-1}]	Volumetric Energy Density [Wh l^{-1}]	Power Density [W l^{-1}]
A-aMEGO/BMIM BF_4/AN	1.15	137	99	158	58	42	67	119
A-aMEGO/EMIM TFSI/AN	1.15	154	104	177	66	45	75	130
aMEGO/BMIM BF_4/AN[8]	0.34	165	49	56	70	21	24	85
Compressed aMEGO/ BMIM BF_4/AN[10]	0.75	147	70	110	63	34	48	17

results in increased bulk density of the electrode and hence the volumetric capacitance values for A-aMEGO samples are significantly higher than the reported values for carbon-based electrodes in the literature.[8,10–27]

The device performance in long term cycling was investigated at a rate of 5 A g^{-1} and a maximum voltage of 3.5 V for 5000 cycles. The specific capacitance retention as a function of cycle number for the electrodes with BMIM BF_4/AN is presented in Figure 3b. After a small decrease of specific capacitance in the first 1000 cycles, its retention value stayed nearly constant at 94% during 5000 cycles. For the electrodes with EMIM TFSI/AN, a similar trend was observed and the retention value was also 94% after 5000 cycles (Figure S4). This again confirms that there are no electrochemical reactions involved in the capacitance process and also the pore accessibility for the aligned activated MEGO does not change by cycling.[26,28–30]

Energy density and power density, as two governing metrics of supercapacitors, were investigated using the values obtained from galvanostatic experiments. The volumetric energy density for the A-aMEGO electrodes with BMIM BF_4/AN from the data at 1 A g^{-1} was 67.0 Wh l^{-1}. For samples with EMIM TFSI/AN the volumetric energy density was found to be 75.3 Wh l^{-1}. Increasing the discharge rate did not considerably influence the performance of the device in terms of energy density. The volumetric energy density values were found to be 65.1 Wh l^{-1} and 63.2 Wh l^{-1}for electrodes with BMIM BF_4/AN and 72.9 Wh l^{-1} and 70.9 Wh l^{-1}for samples with EMIM TFSI/AN at 3 A g^{-1} and 5 A g^{-1} discharge rates, respectively.

The power density for these samples was calculated from the IR drop. **Figure 4**a compares the volumetric and Figure 4b the traditional gravimetric values (per active material mass only) for power and energy densities. As shown in the Ragone plot in Figure 4a, the volumetric power density values from the data at 1 A g^{-1} rate were 119 kW l^{-1} for the electrodes with BMIM BF_4/AN and 130 kW l^{-1} for the electrodes with EMIM TFSI/AN. These values are remarkably large for supercapacitors based on graphene/ionic liquid combinations and provoked by the dense morphology while maintaining the ordered pathway for ion propagation in the A-aMEGO supercapacitors.[8,13–18,31–37]

These high volumetric energy and power densities render these high bulk density A-aMEGO electrodes suitable candidates for practical large scale applications where an increased amount of this material can be included inside packaged supercapacitor devices. This is depicted in the Ragone plot in Figure S5 where the energy and power densities are plotted in terms of per total weight of the electrode (active material and electrolyte). A-aMEGO samples exhibit the highest energy and power densities per total electrode weight compared to the ones reported in the literature.

Understanding of the ion diffusion in the A-aMEGO electrodes was obtained by conducting electrochemical impedance spectroscopy measurements in the frequency range of 10 mHz to 1 MHz and using DC bias voltages of 2.5 and 3.5 V, respectively to evaluate the impedance dependency on the voltage. **Figure 5**a shows the Nyquist plot for the electrodes containing BMIM BF_4/AN and the inset in the figure shows the high frequency region of the Nyquist plot. Regardless of the bias voltage,

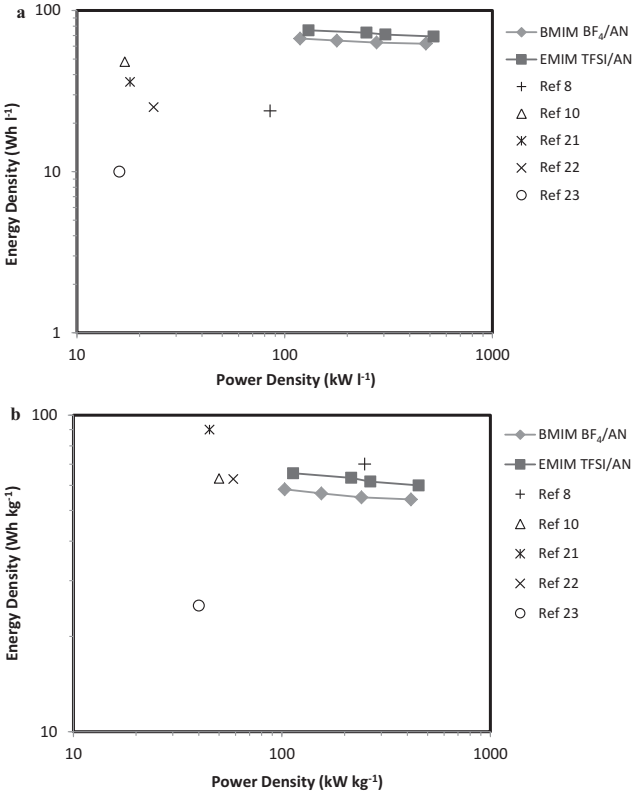

Figure 4. Ragone plot for A-aMEGO samples along with the highest reported values for graphene/ionic liquid combinations under similar voltage and discharge current values. (a) Volumetric values and (b) gravimetric values (per active material weight).

Adv. Mater. **2013**,
DOI: 10.1002/adma.201301243

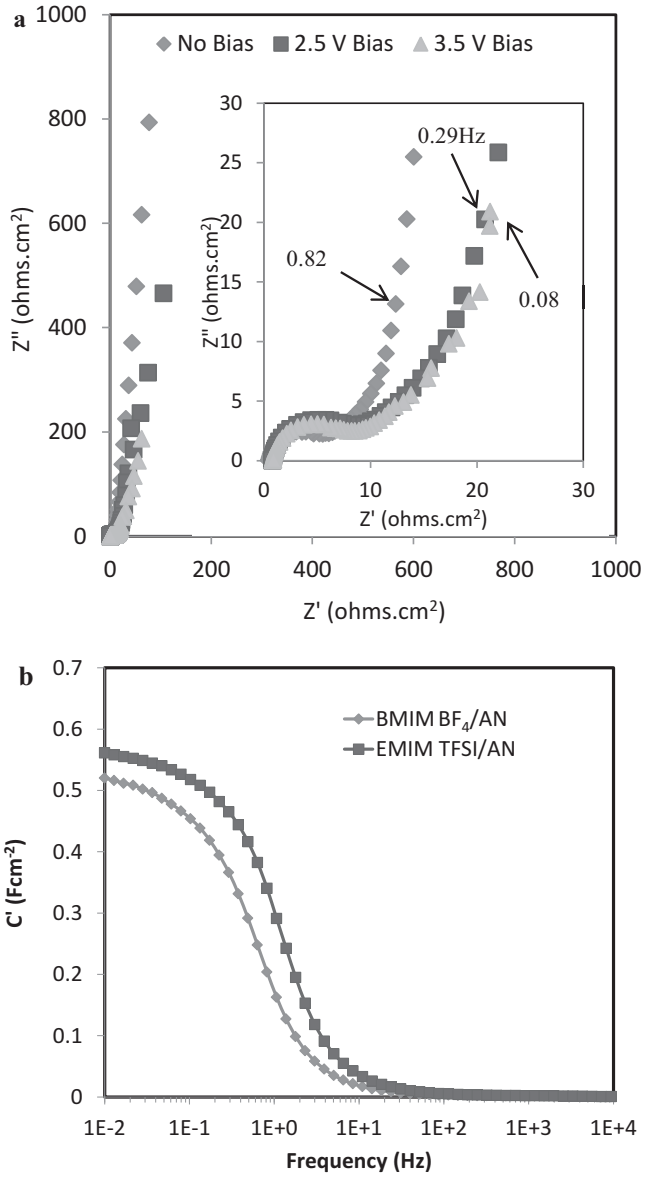

Figure 5. (a) Nyquist plot for A-aMEGO samples at 10 mHz to 1 MHz frequency range and no DC potential, 2.5 V and 3.5 V DC bias. The inset is the data for high frequency region. Arrows show the frequency where $Z'=Z''$. (b) Real part of capacitance as a function of frequency, indicative of the high dependent capacitance at low frequencies.

the Nyquist plot has a similar shape for all three measurements with all the plots showing a steep rise in the imaginary axis at low frequency which is a characteristic of the capacitive behavior (the imaginary part of the electric impedance is much larger than the real part of the electric impedance). At high frequency region, similar shapes with a slight increase in the high frequency resistance with the bias voltage were observed, indicating an increased resistive behavior of the electrode with the bias voltage. In the middle frequency range of the Nyquist plot, ion migration in the electrode can be investigated and the effect of electrode porosity and thickness on this migration can be studied.[4,30] Additionally, the imaginary part of the impedance (in absolute value) decreases with the DC bias voltage. This result indicates that the capacitance value increases with the DC bias voltage, and this increase can be interpreted as a result of the increase in the dielectric constant of the electrolyte or the decrease in the charge separation distance induced by applying bias potential. This confirms that the charge storage takes place nearly exclusively in the double layer and no evident electrochemical reaction takes place under 3.5 V DC bias voltage.[38–39]

Very similar behavior was observed for the A-aMEGO electrodes with EMIM TFSI/AN (Figure S6) with slightly lower resistive behavior for the sample with EMIM TFSI/AN. Since both A-aMEGO electrodes have a similar nano-morphology, this reduction in the resistance can be attributed to the higher ionic mobility of EMIM TFSI/AN in the A-aMEGO pores compared with that of BMIM BF_4/AN (similar to the ESR results from charge/discharge cycles). The higher ion conductivity of EMIM TFSI/AN in A-aMEGO samples can also be observed at the high frequency range as it shows lower resistance compared to the electrodes with BMIM BF_4/AN. The high frequency resistance under open circuit condition was calculated to be 8.37 Ω for BMIM BF_4/AN and 6.27 Ω for EMIM TFSI/AN sample.

The real part of capacitances (C') as a function of frequency for the A-aMEGO electrodes are presented in Figure 5b. The capacitance value at low frequencies for the electrodes containing EMIM TFSI/AN was higher compared to that with BMIM BF_4/AN, which is consistent with the slightly higher capacitance and energy density obtained from galvanostatic experiments for this sample.

The frequency dependence of the imaginary part of the capacitance provides information about the speed by which a capacitor can deliver its energy. This plot for the A-aMEGO samples is shown in Figure S7. The time constants for these samples were found to be 3.65 s for BMIM BF_4/AN and 2.51 s for EMIM TFSI/AN, which is consistent with the faster discharge rate and therefore higher power density for the sample containing EMIM TFSI/AN as an electrolyte. In addition, these time constants are very close to those from low bulk density aMEGO electrodes.[8,10,29,30]

In summary, aligned nano-porous aMEGO electrodes were fabricated using a vacuum-assisted self-assembly process followed by slow infiltration of PTFE binders which led to a tremendous bulk density of 1.15 g cm^{-3}. The experimental results revealed the near optimal nano-morphology of the electrodes which eliminates the micrometer-sized pores (presented in the carbon based electrodes using traditional fabrication methods and do not contribute to the energy storage, therefore reduce the volumetric energy density of the devices) while maintaining a high degree of nanometer-sized pores that are responsible for the formation of an electric double layer and energy storage. Very high volumetric capacitance of 158 F cm^{-3} for the A-aMEGO with BMIM BF_4/AN and 177 F cm^{-3} for the sample with EMIM TFSI/AN as electrolyte were obtained. The gravimetric capacitance in terms of the mass of the active material was 137 F g^{-1} for the A-aMEGO with BMIM BF_4/AN and 154 F g^{-1} for sample with EMIM TFSI/AN as electrolyte, which are slightly lower than that (165 F g^{-1} and 200 F g^{-1} for the two electrolytes, respectively) obtained from the aMEGO electrodes using the traditional fabrication method.[8,10] The A-aMEGO electrodes exhibited very high volumetric energy densities of

67.0 Wh L^{-1} and 75.3 Wh L^{-1} and power densities of 119 kW L^{-1} and 130 kW L^{-1} using BMIM BF_4/AN and EMIM TFSI/AN, respectively. The outsatnding volumetric performance of the A-aMEGO electrodes introduces a realistic energy storage device configuration to meet various technological demands.

Experimental Section

Synthesis of nanoporous microwave exfoliated graphite oxide (aMEGO): *a*MEGO was prepared by activation of graphite oxide via a technique that has been reported in Ref. 8. Briefly, microwave exfoliated graphite oxide (200 mg) was mixed with a 7 M solution (10 mL) of KOH for 24 h. After filtration and drying of the mixture, the solid part was activated at 800 °C in a tube furnace under an argon flow for 1 h. Finally, the mixture was washed with de-ionized water until neutral pH, followed by thermal annealing under 1100 °C to remove any residual functional groups containing oxygen, such as carboxylic acid and hydroxyl groups.

Preparation of A-aMEGO: To fabricate high density aligned aMEGO electrodes, aMEGO was dispersed in N,N-dimethylformamide (DMF, Aldrich) and the mixture was vacuum filtered using a Buchner funnel and an Anodisc filter paper (Whatman, 0.02 μm pore size). During this filtration process, aMEGO layers are pulled towards the Anodisc surface and these layers of nano-porous microwave exfoliated graphite oxide stack successively on top of each other[40]. The thickness of the prepared samples was between 90 to 100 μm. Then, the A-aMEGO disk was air dried for 2 h and vacuum dried at 110 °C for 24 h before the experiments.

Fabrication of the device: In this study, 10 wt% poly(tetrafluoroethylene) (PTFE) was used as binder. In order to infiltrate PTFE into the A-aMEGO structure, a commercially available 60 wt% dispersion of PTFE in water (Aldrich) was used to prepare a very dilute (0.6 wt%) dispersion of this polymer in a 50/50 water/isopropyl alcohol (Aldrich) mixture. Then, an appropriate amount of this dispersion was added to an A-aMEGO disk and was left for a week for efficient and uniform PTFE infiltration and well-controlled solvent removal. Finally the disk was annealed at 140 °C. The electrodes with 3mm lateral dimensions were cut and used for measurements. For electrochemical characterization, the samples were soaked in 2M solutions of 1-butyl-3-methyl-imidazolium tetrafluoroborate (BMIM BF_4) or 1-ethyl-3-methyl-imidazolium bis (trifluoromethylsulfonyl) imide (EMIM TFSI) (Iolitec) in acetonitrile (AN; Aldrich) and a three-layer capacitor composed of A-aMEGO electrode/polypropylene separator (Celgard 3501)/A-aMEGO electrode was prepared. This capacitor was then sandwiched between two gold current collectors and finally two stainless steel electrodes. All samples were baked at 110 °C for minimum of 72 h in order to remove any residual moisture or other volatile impurities prior to measurements.

Characterization: Scanning electron microscopy images were acquired using an FEI NanoSEM 630 FESEM. The porous characteristics of A-aMEGO electrodes were obtained by N_2 adsorption/desorption experiments at 77.1 K using ASAP 2020 V4.00 (V4.00 H). The specific surface area (SSA) was measured according to the Brunauer–Emmett–Teller (BET) method and the pore size distribution was calculated using the non-local density functional theory (NLDFT). Electrochemical experiments on the A-aMEGO-based supercapacitors were carried out using a two electrode system under an inert nitrogen filled glove box controlled environment. The electrochemical performance was evaluated by cyclic voltammetry measurements using a Princeton Applied Research Versastat 4 potentiostat at 5, 20, and 100 mV s^{-1} scan rates and a maximum voltage of 3.5 V. The same equipment was used to investigate the galvanostatic charge/discharge behavior of the samples at 1, 3, 5 and 10 Ag^{-1} discharge rates and a maximum voltage of 3.5 V. The gravimetric capacitance (per active material only) values were calculated from

$$C = \frac{4I}{M\left(\frac{\Delta V}{\Delta t}\right)} \quad (1)$$

where I is the constant discharge current, M is the active material mass for both electrodes, and $\Delta V/\Delta t$ is the slope of the discharge curve after the IR drop. The volumetric values were calculated by multiplying the gravimetric values by 1.15, the density of the A-aMEGO electrodes. Using the values for the capacitance, the energy density was calculated using

$$E = \frac{1}{8} C (\Delta V)^2 \quad (2)$$

where ΔV is the discharge potential window. Power density was calculated by

$$P = \frac{(\Delta V)^2}{4ESR} \quad (3)$$

where *ESR* is the equivalent series resistance from the IR drop in galvanostatic charge/discharge test. Electrochemical Impedance Spectroscopy (EIS) was performed by a Princeton Applied Research PARSTAT 2273 potentiostat over a frequency range from 10 mHz to 1 MHz. EIS experiments were carried out both at open circuit voltage as well as at DC bias potentials of 2.5 V and 3.5 V with a 5 mV AC signal amplitude. From the impedance data, both the real and imaginary capacitance can be obtained as,

$$C^{\uparrow\prime}(\omega) = \left(-Z''(\omega)\right) / \left(\omega |Z(\omega)|^{\uparrow}2\right) \quad (4)$$

$$C^{\uparrow''}(\omega) = \left(Z\uparrow'(\omega)\right) / \left(\omega |Z(\omega)|^{\uparrow}2\right) \quad (5)$$

where Z' and Z'' are the real and imaginary parts of the impedance as a function of frequency (ω), respectively. $|Z(\omega)|^{\uparrow}2 = [\![Z\prime]\!]^{\uparrow}2 + Z^{\uparrow\prime\prime}2$ [29, 41, 42].

Supporting Information

Supporting Information is available from the Wiley Online Library or from the author.

Acknowledgements

The work at Penn State was supported by NSF under grant number CMMI-1130437(MG) and AFOSR under grant number FA9550-11-1-0192 (YZ, ML and QMZ). RSR appreciates support from the U.S. Department of Energy (DOE) under award DE-SC0001951.

Received: March 18, 2013
Revised: April 26, 2013
Published online:

[1] J.R. Miller, P. Simon, *Science* **2008**, *321*, 651.
[2] B. Chu, X. Zhou, K. Ren, B. Neese, M. Lin, Q. Wang, F. Bauer, Q. M. Zhang, *Science* **2006**, *313*, 334.
[3] A. Burke, *Electrochim. Acta* **2007**, *53*, 1083.
[4] B. E. Conway, *Electrochemical Supercapacitors: Scientific Fundamentals and Technological Applications*; Kluwer Academic/Plenum Publisher: New York, **1999**.
[5] V. V. N. Obreja, *Physica. E* **2008**, *40*, 2596.
[6] E. Frackowiak, F. Beguin, *Carbon* **2001**, *39*, 937.
[7] E. Frackowiak, F. Beguin, *Carbon* **2002**, *40*, 1775.
[8] Y. Zhu, S. Murali, M. D. Stoller, K. J. Ganesh, W. Cai, P. J. Ferreira, A. Pirkle, R. M. Wallace, K. A. Cychosz, M. Thommes, S. Dong, E. A. Stach, R. S. Ruoff, *Science* **2011**, *332*, 1538.

DOI: 10.1002/adma.201301243

[9] Y. Gogotsi, P. Simon, *Science* **2011**, *334*, 917.
[10] S. Murali, N. Quarles, L. L. Zhang, J. R. Potts, Z. Tan, Y. Lu, Y. Zhu, R. S. Ruoff, *Nano Energy* **2013**, DOI 10.1016/j.nanoen.2013.01.007.
[11] P. Simon, Y. Gogotsi, *Nat. Mater.* **2008**, *7*, 845.
[12] D. N. Futaba, K. Hata, T. Yamada, T. Hiraoka, Y. Hayamizu, Y. Kakudate, O. Tanaike, H. Hatori, M. Yumura, S. Iijima, *Nat. Mater.* **2006**, *5*, 987.
[13] Y. Wang, Z. Q. Shi, Y. Huang, Y. F. Ma, C. Y. Wang, M. M. Chen, Y. S. Chen, *J. Phys. Chem. C* **2009**, *113*, 13103.
[14] M. D. Stoller, C. W. Magnuson, Y. Zhu, S. Murali, J. W. Suk, R. Piner, R. S. Ruoff, *Energy Environ. Sci.* **2011**, *4*, 4685.
[15] O. Barbieri, K. Hahn, A. Herzog, R. Kotz, *Carbon* **2005**, *43*, 1303.
[16] A. Izadi-Najafabadi, S. Yasuda, K. Kobashi, T. Yamada, D. N. Futaba, H. Hatori, M. Yumura, S. Iijima, K. Hata, *Adv. Mater.* **2010**, *22*, E235.
[17] M. D. Stoller, S. J. Park, Y. W. Zhu, J. H. An, R. S. Ruoff, *Nano Lett.* **2008**, *8*, 3498.
[18] D. W. Wang, F. Li, J. P. Zhao, W. C. Ren, Z. G. Chen, J. Tan, Z. S. Wu, I. Gentle, G. Q. Lu, H. M. Cheng, *ACS Nano* **2009**, *3*, 1745.
[19] Y. Q. Sun, Q. O. Wu, G. Q. Shi, *Energy Environ. Sci.* **2011**, *4*, 1113.
[20] M. Pumera, *Energy Environ. Sci.* **2011**, *4*, 668.
[21] C. Liu, Z. Yu, D. Neff, A. Zhamu, B. Z. Jang, *Nano Lett.* **2010**, *10*, 4863.
[22] Q. Cheng, J. Tang, J. Ma, H. Zhang, N. Shinya, L. Qin, *Phys. Chem. Chem. Phys.* **2011**, *13*, 17615.
[23] Y. Zhu, L. Li, C. Zhang, G. Casillas, Z. Sun, Z. Yan, G. Ruan, Z. Peng, A. O. Raji, C. Kittrell, R. H. Hauge, J. M. Tour, *Nature Communications* **2012**, *3*, 1225.
[24] P. C. Chen, G. Shen, Y. Shi, H. Chen, C. Zhou, *ACS Nano* **2010**, *4*, 4403.
[25] C. Peng, S. W. Zhang, X. H. Zhou G. Z. Chen, *Energy Environ. Sci.* **2010**, *3*, 1499.
[26] J. Chmiola, C. Largeot, P. L. Taberna, P. Simon, Y. Gogotsi, *Science* **2010**, *328*, 480.
[27] P. Simon, Y. Gogotsi, *Accounts of Chemical Research* **2012**.
[28] G. Srinivas, J. Burress, T. Yildirim, *Energy Environ. Sci.* **2012**, *5*, 6453.
[29] P. L. Taberna, P. Simon, J. F. Fauvarque, *J. Electrochem. Soc.* **2003**, *150*, A292.
[30] Y. Liu, R. Zhao, M. Ghaffari, J. Lin, S. Liu, H. Cebeci, R. G. de Villoria, R. Montazami, D. Wang, B. L. Wardle, J. R. Heflin, Q. M. Zhang, *Sensor. Actuat. A-Phys* **2012**, *181*, 70.
[31] T. Y. Kim, H. W. Lee, M. Stoller, D. R. Dreyer, C. W. Bielawski, R. S. Ruo, K. S. Suh, *ACS Nano* **2011**, *5*, 436.
[32] J. Zhang, J. Jiang, H. Li, X. S. Zhao, *Energy Environ. Sci.* **2011**, *4*, 4009.
[33] Z. S. Wu, W. Ren, D. W. Wang, F. Li, B. Liu, H. M. Cheng, *ACS Nano* **2010**, *4*, 5835.
[34] Q. Cheng, J. Tang, J. Ma, H. Zhang, N. Shinya, L. C. Qin, *Carbon* **2011**, *49*, 2917.
[35] J. Segalini, B. Daffos, P.L. Taberna, Y. Gogotsi, P. Simon, *Electrochim. Acta* **2010**, *55*, 7489.
[36] R. Lin, P.L. Taberna, J. Chmiola, D. Guay, Y. Gogotsi, P. Simon, *J. Electrochem. Soc.* **2009**, *156*, A7.
[37] A. Jänes, L. Permann, P. Nigu, E. Lust, *Surf. Sci.* **2004**, *560*, 145.
[38] E. Frackowiak, K. Metenier, V. Bertagna, F. Beguin, *Appl. Phys. Lett.* **2000**, *77*, 2421.
[39] W. Lajnef, J. M. Vinassa, O. Briat, S. Azzopardi, E. Woirgard, *J. Power Sources* **2007**, *168*, 553.
[40] Q. Liang, X. Yao, W. Wang, Y. Liu, C. P. Wong, *ACS Nano* **2011**, *5*, 2392.
[41] D. Qu, H. Shi, *J. Power Sources* **1998**, *74*, 99.
[42] H. K. Song, Y. H. Jung, K. H. Lee, L. H. Dao, *Electrochim. Acta* **1999**, *44*, 3513.